

Gap Filling of Net Ecosystem CO₂ Exchange (NEE) above Rain-Fed Maize Using Artificial Neural Networks (ANNs)

Babak Safa^{1*}, Timothy J. Arkebauer², Qiuming Zhu³, Andy Suyker⁴, Suat Irmak⁵

¹Daugherty Water for Food Global Institute at the University of Nebraska, Lincoln, USA

²Department of Agronomy & Horticulture, University of Nebraska-Lincoln, Lincoln, USA

³Department of Computer Science, University of Nebraska-Omaha, Omaha, USA

⁴School of Natural Resources, University of Nebraska-Lincoln, Lincoln, USA

⁵Biological Systems Engineering Department, University of Nebraska-Lincoln, Lincoln, USA

Email: *s-bsafal@unl.edu

How to cite this paper: Safa, B., Arkebauer, T.J., Zhu, Q.M., Suyker, A. and Irmak, S. (2021) Gap Filling of Net Ecosystem CO₂ Exchange (NEE) above Rain-Fed Maize Using Artificial Neural Networks (ANNs). *Journal of Software Engineering and Applications*, 14, 150-171.

<https://doi.org/10.4236/jsea.2021.145010>

Received: March 4, 2021

Accepted: May 23, 2021

Published: May 26, 2021

Copyright © 2021 by author(s) and Scientific Research Publishing Inc.

This work is licensed under the Creative Commons Attribution International License (CC BY 4.0).

<http://creativecommons.org/licenses/by/4.0/>



Open Access

Abstract

The eddy covariance technique is an accurate and direct tool to measure the Net Ecosystem Exchange (NEE) of carbon dioxide. However, sometimes conditions are not amenable to measurements using this technique. Thus, different methods have been developed to allow gap-filling and quality assessment of eddy covariance data sets. In this study first, two different Artificial Neural Networks (ANNs) approaches, the Multi-layer Perceptron (MLP) trained by the Back-Propagation (BP) algorithm, and the Radial Basis Function (RBF), were used to fill missing NEE data measured above rain-fed maize at the University of Nebraska-Lincoln Agricultural Research and Development Center near Mead, Nebraska. The gap-filled data were then compared by different statistical indices to gap-filled data obtained with the technique suggested by Suyker and Verma in 2005 [S&V method], and the ANN approach presented by Papale in 2003. The results showed that the RBF network was able to find better fits for missing values compared to the MLP (BP) network and S&V method. In addition, unlike the S&V method, which depends on different gap-filling procedures over the year; the structure of RBF and MLP (BP) networks was constant. However, data analysis indicated Papale's approach gave better fits than the RBF and MLP (BP) methods. Thus, based on this work, Papale's approach is the best method to estimate the missing data; though the applied statistical indices, which were used for model evaluation, show little difference between Papale's approach and the RBF and MLP (BP).

Keywords

Gap Filling, Net Ecosystem Exchange of Carbon Dioxide, Artificial Neural Networks, Eddy Covariance System

1. Introduction

The eddy covariance technique is one of the most accurate and direct tools to help us measure the carbon exchange between the surface and the atmosphere in various ecosystems.

Most often eddy covariance data quality has problems, as a result of instrument malfunctions, power outage, extreme weather conditions, and insufficient turbulent mixing [1] [2] [3]. The annual average of missing values has been reported to range from 30% to 45% [2] and even as high as 65% [4].

Stable conditions and low turbulence are factors that result in under-estimation of daily NEE. Since these conditions often occur at night the Net Ecosystem Exchange (NEE) values are removed when the measured wind speeds are less than a threshold friction velocity (u^*) [5].

To fill missing data, various methods are applied such as non-linear regressions, dual unscented Kalman filter, semi-parametric models, terrestrial biosphere models, and artificial neural networks [1]-[6]. The comparison of several approaches by [6] indicated that Artificial Neural Networks (ANNs) have some advantages such as their performance without the underlying assumptions in mechanistic models, and the capability to provide a good estimation in different ecosystems.

Although intensive efforts in gap-filling methods have already been made, there is a necessity for conducting more research in order to establish the accuracy and reliability of the techniques based on variability in plant, climate, and particularly, the quality and quantity of the data set.

In this study, first, we investigated the function of two different ANN methods known as the Multi-layer Perceptron (MLP) trained by the Back-propagation (BP) algorithm and the Radial Basis Function (RBF) in order to fill the missing NEE data for rain-fed maize. Then, the gap-filled data, using mentioned methods, were compared with the technique suggested by Verma & Suyker (V&S) [7] and the ANN method presented by [8]. The method applied by Verma & Suyker has been accepted as a basic approach for the AmeriFlux sites at Mead, Nebraska and Papale's approach has been recently utilized for filling the data gaps by scientists in the AmeriFlux community.

2. Methodology

1) *Artificial neural networks*

Artificial Neural Networks (ANNs) are dynamic systems, which can compute and identify the relationships among input and output data to obtain estimation

with the best approximation [9]. ANNs are composed of simple interconnected processing elements (PEs), called neurons, which operate in parallel. They endeavor to make a model that is similar to the neuro-synaptic structure of the brain [9]. An artificial neuron, like its biological counterpart, is comprised of input vectors (P) which are analogous to dendrites, weight vectors (w) which are similar to synaptic junctions, bias vector (b) which represent the least stimulation threshold, an activation function (f) that mimics soma function, and an output vector (a) that is analogous to the axon (Figure 1).

Today, ANNs are powerful tools that can approximate many complex phenomena. They were trained to perform pattern recognition, identification, classification, and control systems. ANNs are particularly suited to fill data gaps for NEE flux using other sources of data [2] [6] [10].

2) Multi-layer perceptron network:

Multi-layer Perceptron (MLP) Networks are feed-forward neural networks containing input layers, an output layer, and one or more hidden layers. An MLP is a fully connected network (Figure 2). In other words, each neuron in each layer is entirely connected to neurons in the previous or next layer. The weight and bias parameters are adjusted by the activation function and learning rule. The activation functions in hidden layers are usually tangent hyperbolic or sigmoid, whereas, in the output layer, the application of a linear function is recommended. The learning rule is a procedure, which the network parameters are adjusted in order to obtain a specific function, which can map the input vector to the output vector.

The best systematic method for training MLP networks is the Steepest Descent Back-propagation, organizing two main paths, forward and backward (Safa *et al.*, 2011). In the forward path, the input vector is applied through the MLP network and its effects, via the hidden layer, are distributed onto the output layer without any change in the network parameters. In the backward path, unlike the first one, all network parameters change and are adjusted by the error correction rule. An error vector is formed in the output layer and is taken into account by the difference between the actual (observed) and estimated values. The error values from the output layer are distributed in the entire network. This process is continued until the amount of error becomes as low as possible and stability is observed in network parameters.

Equations (1) and (2) respectively, show the adjustment process in the output and hidden layers (Kumar *et al.*, 2002):

$$w(N+1) = w(N) - \eta \delta \phi \quad (1)$$

$$w(N+1) = w(N) + \eta \chi \sum_{q=1}^r \delta_q \quad (2)$$

where; w is weight, N the number of iteration, χ input value, η learning rate, ϕ output, and δ is defined as $2\varepsilon_q \partial \phi / \partial I$, I the sum of the weighted inputs, q neuron index of the output layer, and ε_q error signal.

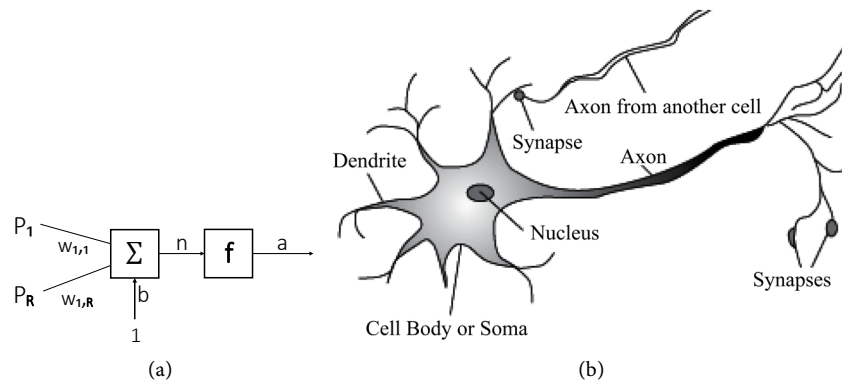


Figure 1. Model of single neuron (a) Artificial (b) Biological.

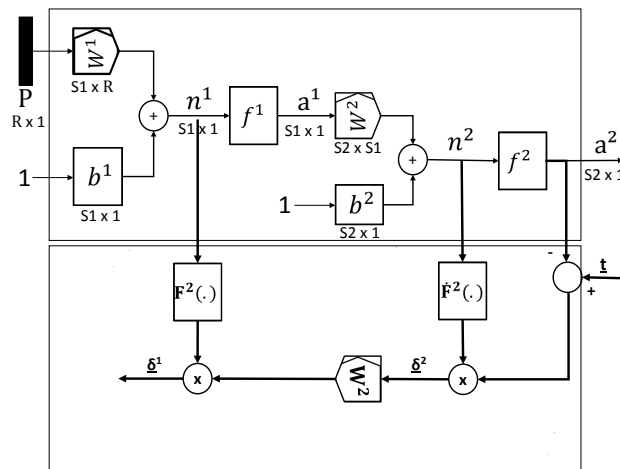


Figure 2. Steepest Descent Back-Propagation Algorithm at a MLP network with one hidden layer.

The learning rate (η) determines the step span on the activation function over each repetition of network parameters optimization. If lower values of the learning rate are selected, the changes in the network parameters will be smaller after each repetition, a case that will help to smooth the movement path of parameters toward the optimum quantities and will slow down the learning process. Inversely, when the learning rate is increased, although the learning speed is increased too, large changes are made from one repetition to the next, which occasionally will bring instability in the network situation generally referred to as divergent network parameters [9].

The momentum parameters can help to avoid this problem. Momentum is defined as the amount of inertia that is increased in each network parameter. It is utilized to improve the learning rate and prevents instability in the network [11]. Therefore, to modify the Back-propagation algorithm using a momentum term, the change of weight parameter is computed as follows [12]:

$$\Delta w(N+1) = -\eta\delta\phi + \mu\Delta w(N) \tag{3}$$

where; μ is momentum coefficient and $\Delta w(N+1)$ the change of weight during N to $N+1$ learning cycles.

One of the other network parameters is epoch. One entire set of inputs which is given to the network at each learning cycle is called an epoch.

3) *Radial basis function networks:*

A Radial Basis Function (RBF) network is a fully inter-connected feed-forward structure composed of three layers (input, hidden, and output). The activation function in hidden neurons is a Gaussian exponential whereas, in the output layer, it is a linear function. The Gaussian function consists of two main parameters, center (c) and width (σ). In each neuron in the hidden layer, the Euclidean (radial) distance $(x - c)$ is computed where x is input vector, and c is the prototype vector, which represents the center of RBF.

The output value for the hidden layer (Figure 3) is computed by:

$$h_j^p = R_j^p / \sum_{j=1}^L R_j^p \quad (p = 1, 2, \dots, P), (j = 1, 2, \dots, M)$$

$$R_j^p = \exp \left[-\frac{1}{2\sigma_j} \sum_{k=1}^N (x_k^p - c_{jk})^2 \right]$$

Furthermore, the output of the output layer is computed by:

$$y_i^p = w_{oj} \sum_{j=1}^L w_{ij} h_j^p$$

where, N , L , and M are the number of units in input, hidden, and output layers; respectively, and P is the number of input patterns, R_j^p is the hidden layer activation function, h_j^p is the normalization of the hidden layer activation function.

RBF networks are trained using supervised and unsupervised learning [13] [14] [15] [16] [17]. In the unsupervised learning phase, the centers and widths of RBF are determined. First, the center (c_{ij}) of the basis function (c_j), using the K-means algorithm, and according to the input data similarities, are clustered in a finite number of samples so that the first L data is selected as an initial value for the center of first cluster. Then, all samples (c_j) modes (M_j) are classified in different groups based on the nearest center. $\sum_{k=1}^n (x_k^p - c_{jk})^2$ is the minimum for all sample modes and basis function where, $x^p = (x_1^p, \dots, x_n^p)$ and x^p belongs to the subset of c_j . c_j is reiterated until a stable cluster formation is obtained.

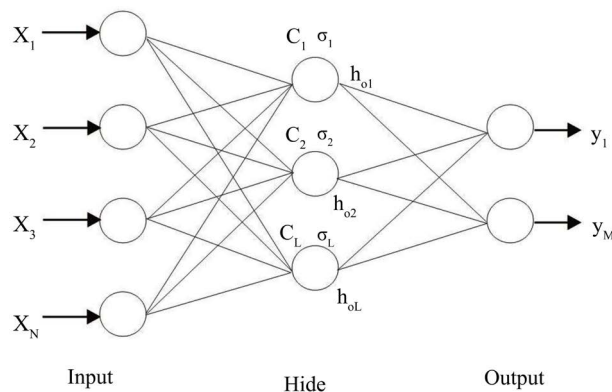


Figure 3. Architecture of a neural network based on RBF.

$$c_{ij} = \frac{1}{M_j} \sum_{p \in \theta_j} x_i^p \quad (4)$$

where, M_j is the number of sample nodes in the sample subset, θ_j . Second, the width (σ_j) of the basis function (c_j) is determined using a P-nearest neighbor method which is expressed by the mean distance between the centers of the basis function and sample nodes in the sample subset:

$$\sigma_j = \sqrt{\frac{1}{M_j} \sum_{p \in \theta_j} \sum_{k=1}^n (x_k^p - c_{jk})^2} \quad (5)$$

In the supervised phase, the weights (θ_j) between hidden layer neurons and the output layer neurons are determined according to the least-squares principle.

$$E_s = \frac{1}{2} \sum_{p=1}^P \sum_{k=1}^M \left(y_k^p - \sum_{j=1}^L w_{jk} h_j^p \right) \quad (6)$$

where, E_s is the function of θ_j and is gotten by least-squares principle, y_k^p is observed output.

RBF networks in comparison with the Back-propagation (BP) networks have some advantages and disadvantages. For instance, they train faster than BP networks with less sensitivity to local minima [10] [18] [19].

One of the major disadvantages of RBF networks is some pre-selection of input data in the hidden neurons, due to the initial learning method during the unsupervised clustering phase, which leads to losing some information contributing to the output neurons [10].

4) Data screening and gap filling procedures using Verma & Suyker's method:

NEE data screening procedures proposed by Verma and Suyker contain four steps: stationarity (NEE data are accepted by criteria discussed by [20]), statistical filtering (removing data when standard deviations of either scalar or velocity fluctuations are outside predetermined limits), nighttime calm winds, and other quality controls (periods when sensors were being calibrated or when flow rate were unacceptable are deleted). The minimum threshold of friction velocity (u^*) was considered to be 0.25 m/s. Their approach for gap filling data is separated into three growth phases: growing season (daytime), growing season (nighttime), and non-growing season (daytime and nighttime). The regression methods that are used to fill the missing NEE values depend on incident photosynthetically active radiation (PAR) for the first phase, air temperature for the second one, and soil temperature for the third one. This approach is utilized at the Mead, Nebraska AmeriFlux sites. The sources of data are at level 2 (Standardized data have been reviewed for consistent units, naming conventions, reporting intervals, and formats. Data can include variables with gaps, or gap-filled and flagged by the tower team) and level 3 (Data obtained by level 2 products. Data are quality checked using standardized techniques and NEE is calculated. Data are not changed but descriptive variables "flag" are added) in the AmeriFlux network.

5) Papalé's approach:

Recently, AmeriFlux scientists at level 4 (Data obtained from level 3 products.

Data are u^* filtered and gap-filled using different methods) have filled in the missing NEE values using the method proposed by [8]. They applied a feed-forward back propagation neural network (BPN) to fill the nighttime values when the absolute threshold of friction velocity (u^*) was considered equal or smaller than 0.2 m/s. This method was used for the first time for four sites in Europe and the results indicated the utility of ANN for gap filling.

6) *Site description and measurements:*

The selected field (Site 3) is located at the University of Nebraska-Lincoln Agricultural Research and Development Center near Mead, NE. According to the Köppen climate classification, Mead has a temperate climate; the mean annual precipitation and temperature (1968-2011) are 719.6 mm and 9.9°C, respectively. Moreover, about 71% of annual precipitation occurs over the growing season (May-October). The soils are deep, silty, clay loams.

Site 3 (41°10'46.8"N, 96°26'22.7"W, 362 m above mean sea level) is not irrigated and during 2001-2009 was planted to a maize-soybean rotation. In this research, the maize years 2001, 2003, 2005, 2007, and 2009 were studied. The ANN method presented by [8] has been utilized for 2001, 2003, and 2005 in AmeriFlux. We therefore studied the same years in this study.

Hourly NEE and the input data were selected from day of year (DOY) 169 to 244 for selected years. To measure NEE flux, an omnidirectional 3D sonic anemometer (R3, Gill Instruments Ltd., Lymington, UK) and a closed path CO₂/H₂O gas analyzer (LI 6262, LI-Cor Inc., Lincoln, NE) were utilized. For sufficient fetch, the sensors were installed 3.0 m above the ground when the canopy was shorter than 1.0 m height, and then moved to 6.0 m height for the remainder of season. Air temperature and vapor pressure at 3.0 m, and 6.0 m were measured with a HMP 35 C (Viasala, Helsinki, Finland). Soil temperature at 0.1 m depth was measured with platinum RTD (Omega Engineering, Stamford, CT). Photosynthetically active radiation was measured with a quantum sensor (LI 190 SA, LI-Cor Inc., Lincoln, NE), and net radiation with a net radiometer (Q*6, REB systems, Seattle, WA). A tipping bucket, TE 525 (Campbell Scientific, Logan, UT), and a cup anemometer (010 C Met One, Instruments, Grants Pass, OR) were used to measure precipitation and wind speed. Soil water content was measured using a ML2x ThetaProbe (Delta-T, Burwell, Cambridge, UK). LAI was determined using a destructive sampling. A LI-3100 (LI-Cor Inc., Lincoln, NE) leaf area meter was used to measure sampled leaves. The period of LAI samplings was generally every 7 to 10 days with due attention that one sampling should be timed to correspond to maximum leaf area index which usually occurs at tasseling.

7) *Data selection:*

To design an ANN, the optimal selection of input elements is a key factor. The understanding of the governing physical and biological laws among input and output elements plays an important role in ANN modeling. Some of the important physiological, meteorological, and edaphic elements that have an effect on

NEE flux include leaf area index (LAI), [m^2/m^2]; soil water content (SWC), in 10 and 25 cm depths; soil temperature (Ts), [$^{\circ}\text{C}$], in 10 cm depth; air temperature (Ta), [$^{\circ}\text{C}$]; vapor pressure deficit (VPD), [kPa]; wind speed (WS), [m/s]; irrigation and precipitation (P), [mm]; net radiation (Rn), [W/m^2]; and the fraction of incoming photosynthetically active radiation (PAR) absorbed by the canopy (fPAR). Furthermore, local time of day, each hour equals 0.0417 (DTime), was added to input elements in order to improve the training of ANN.

8) Gap filling procedures:

Hourly data for twelve input elements accompanied by hourly NEE as output were used in the data matrix architecture (Table 1).

In the matrix, the rows were the calendar years, and the columns were input elements plus output values. After making the data matrix, one year-data (20%) was extracted to make a test file and the others (80%) were applied to the learning file. The year 2005 was selected for the test file. Corresponding to the climatic data records, 2005 had relatively moderate conditions based on precipitation and temperature over the growing season in comparison with the other years. The validation file was developed using the data matrix with NEE observed (screened) values that belonged to the year 2005. This file was not used for training processes. The observed (screened) are data, which after quality control, are recognized to be filled with the new values. In the architecture of MLP networks, three hidden layers networks with the Normalized Cumulative Delta (NCD) rule were used. According to NCD, the adjusted weights at the end of each epoch are stored and the learning rule is independent of the epoch size. The applied activation functions in hidden layers were Tangent Hyperbolic, which ranges in values between $[-1, +1]$. In the output layer, a linear function was used.

The optimum network response was obtained when the epoch chosen was one. The input data were normalized to the interval $[-1, +1]$ which is idiomatically named Bipolar. To design the RBF network using the [21] approach, we used 50 prototype layers with the same parameters as the MLP network.

9) Model evaluation:

Apart from the usual quantitative measures used for the evaluating performance of a model, our study applied the following statistical indices in order to select the best architecture of networks based on the difference between the observed and estimated values.

Root Mean Square Error (RMSE):

$$\text{RMSE} = \sqrt{\frac{1}{n} \sum_{d=1}^n (x_d - \hat{x}_d)^2}$$

Mean Absolute Error (MAE):

$$\text{MAE} = \frac{1}{n} \sum_{d=1}^n |x_d - \hat{x}_d|$$

where x_d is the estimated value, \hat{x}_d the observed value with “ n ” observations.

Table 1. Data matrix architecture.

DOY	Elements	Year	DTime	LAI ^(m²/m²)	SWC (10 cm)	SWC (25 cm)	Ts (10 cm) ^(°C)	Ta ^(°C)	VPD ^{kPa}	p ^(mm)	WS ^(m/s)	Rn ^(W/m²)	APAR pct ^(%)	NEE Flux ^(mg/m²/s) (Output)
169														
170														
171														
...														
242														
243														

3. Results and Discussion

1) *Results of the comparison of NEE flux estimation using the MLP (BP), RBF, and Verma & Suyker's methods.*

After making the data matrix, the training procedures with MLP (BP) and RBF using the initial network parameters for the learning and test file was initiated and continued to achieve the best network parameters based on model evaluation methods. The values of the network parameters used are listed in **Table 2**. There is no remarkable difference among network parameters except of the number of processing elements (PEs) in hidden layers for the RBF network, which is much greater than the MLP network. It is related to the fundamentals of RBF networks.

The quality control of the NEE values for the selected time period in 2005 using Verma & Suyker's approach indicated a number of 468 observed (screened) values that are necessary to be filled by the new data. This dataset formed the validation file. **Table 3** shows the model evaluation according to the computed statistical indices for the validated file. Although there is not a big difference among the statistical indices values, the minimum RMSE was found in the RBF network. Furthermore, the quantities for MAE and e_{\max} (|Maximum Error Value – Minimum Error Value|) also demonstrate that the smallest values were observed for the RBF method. Schmidt [10] confirmed that RBF networks are able to reproduce the NEE missing values better than MLP (BP) networks. In addition, the results show the ability of the estimation of observed (screened) values using Verma & Suyker's approach is more accurate than the MLP network. Thus, the RBF network is evaluated as the best model in order to gap fill data for the NEE.

Figures 4(a)-(c) show that there is no specific pattern between the estimated and observed (screened) NEE values. In other word, a significant difference is observed between the estimated and observed (screened). However, **Figure 4(b)** illustrates the statistical dispersion of the NEE values for the RBF network with respect to the other models is smaller.

Figures 5(a)-(c) depict the dispersion of differences between the estimated and observed (screened) NEE (error) quantities. They indicate no remarkable difference between observed (screened) and estimated NEE for the three applied models though, the e_{\max} has the lowest value for the RBF network (**Table 3**).

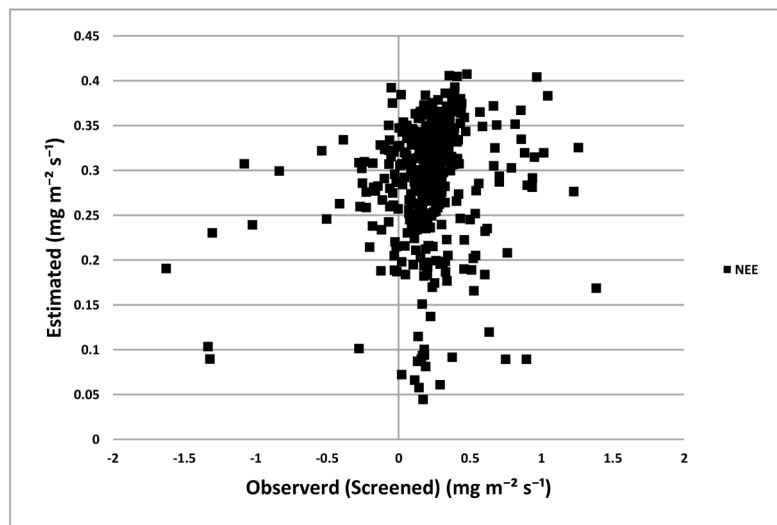
Table 2. Network parameters.

ANNs	# PE in	# PE in	# PE in	# PE in	Learning Coefficient in Momentum			
	input	hidden 1	hidden 2	output	input	hidden 1	hidden 2	output
MLP (BP)	12	24	6	1	0.300	0.200	0.150	0.400
RBF	12	50	34	1	0.300	0.250	0.150	0.400

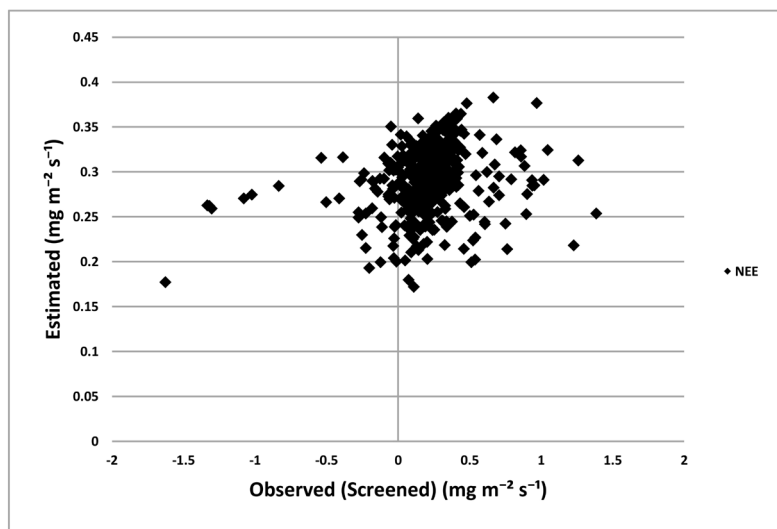
Table 3. Models evaluation.

Models	RMSE ($\text{mg}\cdot\text{m}^{-2}\cdot\text{s}^{-1}$)	MAE ($\text{mg}\cdot\text{m}^{-2}\cdot\text{s}^{-1}$)	e_{\max} ($\text{mg}\cdot\text{m}^{-2}\cdot\text{s}^{-1}$)
MLP (BP)	0.2989	0.1867	3.0342
RBF	0.2970	0.1805	2.9360
V&S	0.2978	0.1825	3.0263

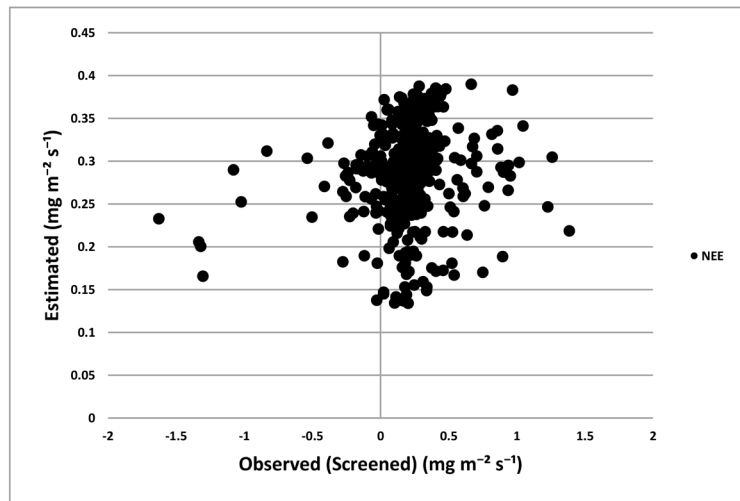
$$e_{\max} = |\text{Maximum Error Value} - \text{Minimum Error Value}|.$$



(a)

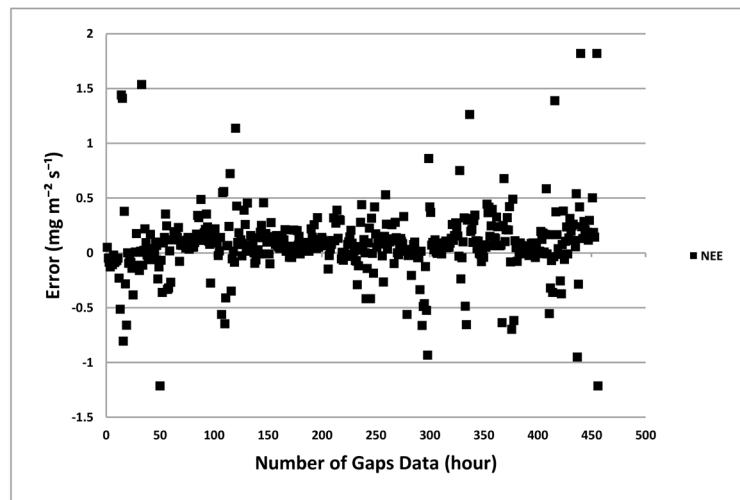


(b)

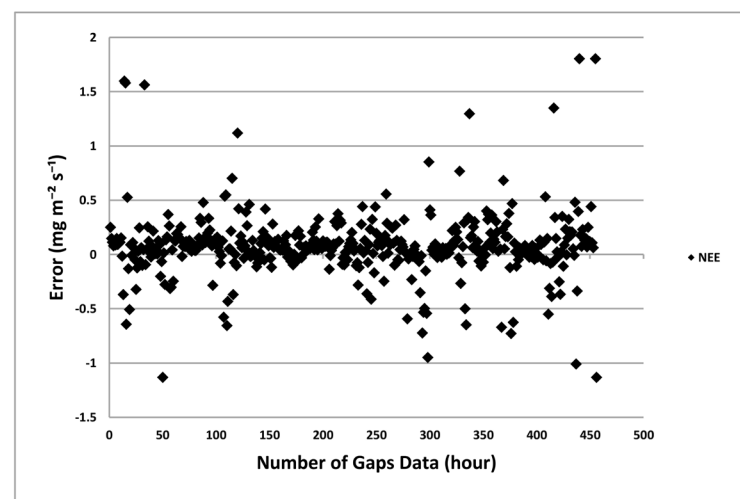


(c)

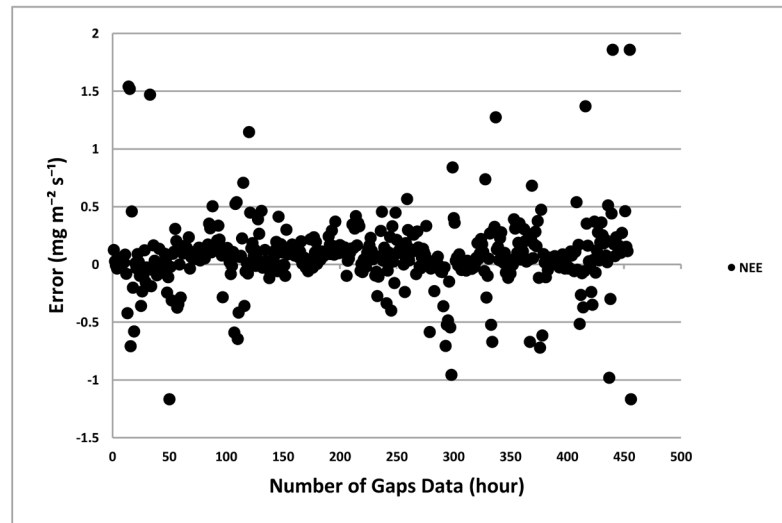
Figure 4. Estimation of NEE for observed (screened) values using (a) MLP (BP), (b) RBF and (c) V&S methods.



(a)



(b)



(c)

Figure 5. The difference (error) between estimated and observed (screened) values of NEE using (a) MLP (BP), (b) RBF and (c) V&S methods.

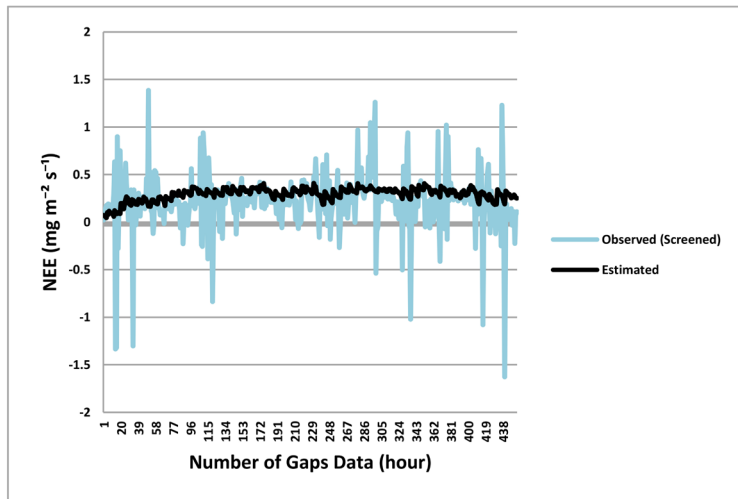
Figures 6(a)-(c) show that there is no consistency between observed (screened) and estimated NEE over the specified time series among the models. Data analysis indicated that the entire gap-filled data belonged to the nighttime hours. Generally, the NEE values must be positive at this moment whereas, they were negative (according to the AmeriFlux network). Moreover, the recorded values mostly contained very large amounts. These irregularities and disturbances in recorded data, lead to a striking disagreement between the observed (screened) and estimated data.

Figures 7(a)-(c) illustrate a short segment (5.5 days) of the NEE variation with the highest reported gap data in 2005 for observed (quality-controlled), estimated, and observed (screened) data using three applied methods. **Figure 7** shows that the total gap-filled values belong to nighttime. Furthermore, a notable difference is seen between estimated and observed (screened) values, which indicates a striking distinction between the observed (screened) and estimated data.

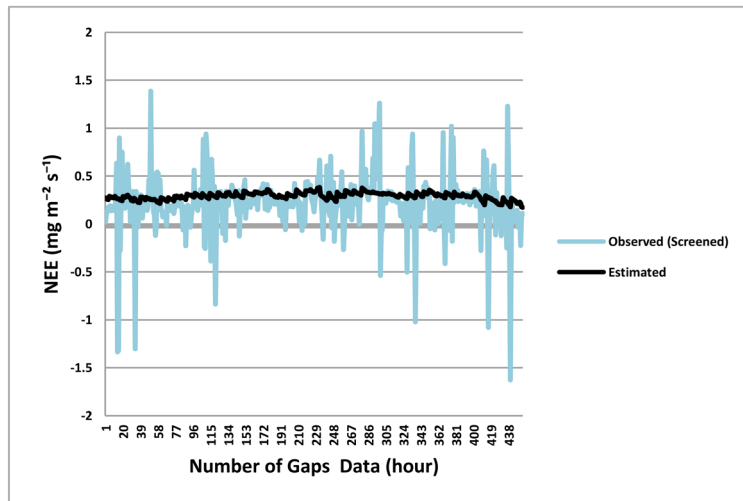
One of the major advantages of the gap-filling procedures using RBF and MLP is that a single computation method is applied throughout a year whereas; Verma & Suyker's gap-filled producers are classified into three time periods. For each of them, the computation method of missing values is different. The study by [6] showed a low annual sum bias for gap-filling performance using an ANN comparing by the other methods such as regression techniques.

Overall, this study suggests that the application of RBF method to fill the gap data in comparison with Verma & Suyker's gap-filled producers is provide values that are more accurate.

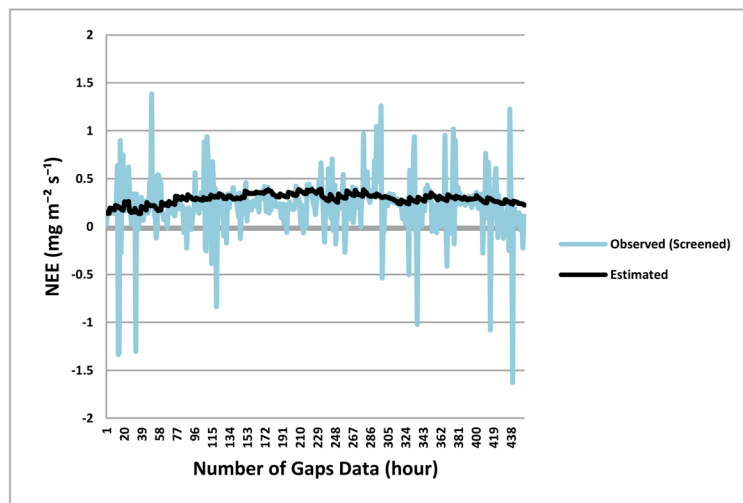
2) *Results of the comparison of NEE flux estimation using the MLP (BP), RBF, and Papale methods.*



(a)

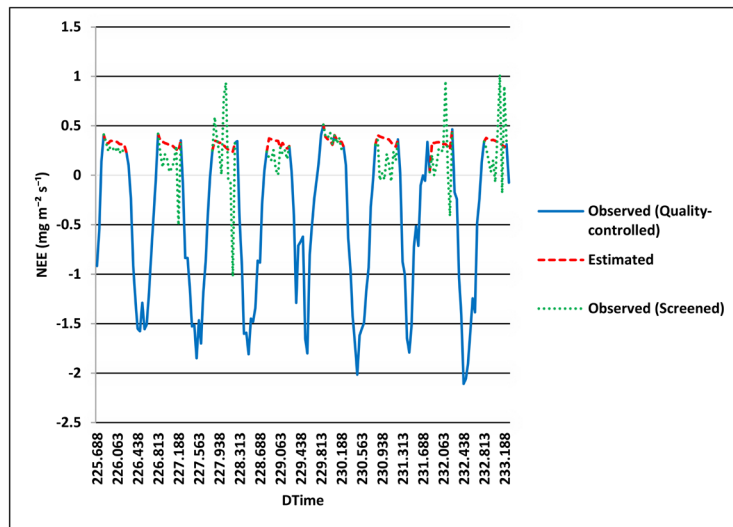


(b)

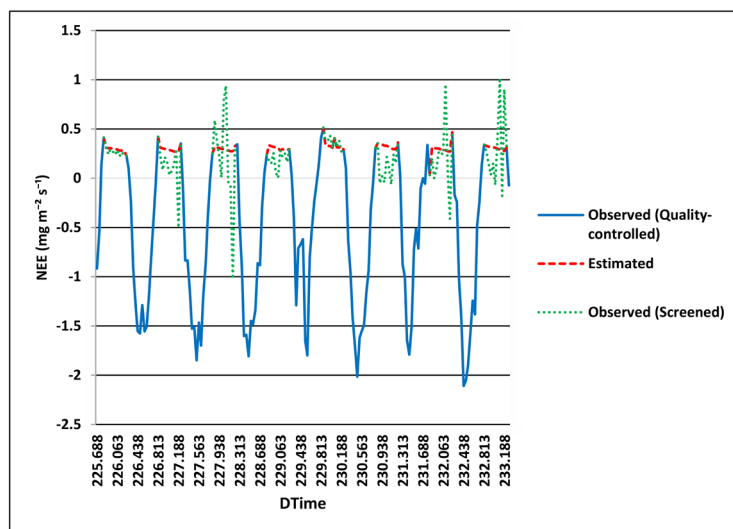


(c)

Figure 6. Comparison of estimated and observed (screened) values of NEE using (a) MLP (BP), (b) RBF and (c) V&S methods.



(a)



(b)

Figure 7. Comparison of the estimated and observed (quality-controlled and screened) values of NEE using (a) MLP (BP), (b) RBF and (c) V&S methods from local time of day 225.688 to 233.271.

Papale's approach has been applied to fill the gap data for the years of 2001 to 2005 by AmeriFlux network. 2005 was selected for making the test data file due to the relatively moderate conditions based on precipitation and temperature over the growing season in comparison with the other years. It is clear that the other years (2001 & 2003) were used to make the data matrix for learning file. Eventually, the networks training procedures using the MLP (BP), RBF, and Papale's methods were accomplished. The network parameters for these methods are shown in **Table 4**. Since the arrangement of the input parameters for both applied networks in sections (a & b) is similar; therefore, the results indicate that there is no remarkable difference between the size of data matrices and network parameters. In other words, the response of MLP (BP) and RBF methods for the two distinc-

tive data matrices which were used for both sections are almost the same.

The quality control of the NEE values for the selected time period in 2005 using Papale's approach indicated a number of 295 observed (screened) values that are necessary to be filled by the new data. This dataset formed the validation file. The model evaluation results according to the error analysis for the validated file are shown in **Table 5**. The smallest values for RMSE, MAE, and e_{\max} belong to Papale's approach. **Table 5** also demonstrates that the evaluation indices indicate the better ability of the RBF network to fill the gap data in comparison with MLP (BP). Thus, it is concluded that according to the evaluation indices Papale's model appears to be the best approach. However, the observed differences among the applied methods are very small. The comparison of fifteen gap-filling techniques for NEE by [6] showed that the two ANNs, an applied feed-forward back propagation neural network by [8], and a stochastic Bayesian network used by [22] had the best performance for gap-filling data in different ecosystems.

The relation between observed (screened) and estimated data is shown in **Figures 8(a)-(c)**. The stronger relationship based on pattern of NEE change was observed in **Figure 8** in respect to **Figure 4**. The reason must be sought through the quality and quantity of data in the test and validated files.

The difference between observed (screened) and estimated NEE is depicted in **Figures 9(a)-(c)**. The lowest dispersion belongs to Papale's method in **Figure 9(c)**. Simultaneously, the e_{\max} has the least value for this method and however, the e_{\max} for the RBF network was very close to it.

Figures 10(a)-(c) depict the comparison of observed (screened) and estimated NEE using the applied three methods. The trend of estimated NEE by Papale and the MLP (BP) approaches have more compatibility with observed (screened) values compared to the RBF method. On the other hand, the fluctuation of estimated values is less than the others in **Figure 10(b)**. It indicates that the estimated results using the RBF method are smoother than the others. The characteristics of data in the test and validated files have resulted in distinct differences among **Figure 10** and **Figure 6**.

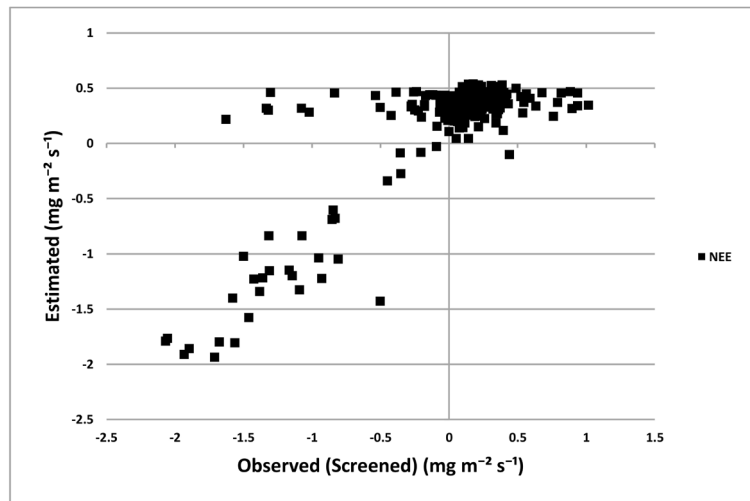
Table 4. Network parameters.

ANNs	# PE in	# PE in	# PE in	# PE in	Learning Coefficient in Momentum			
	input	hidden 1	hidden 2	output	input	hidden 1	hidden 2	output
MLP (BP)	12	28	2	1	0.300	0.200	0.150	0.400
RBF	12	50	31	1	0.300	0.250	0.150	0.400

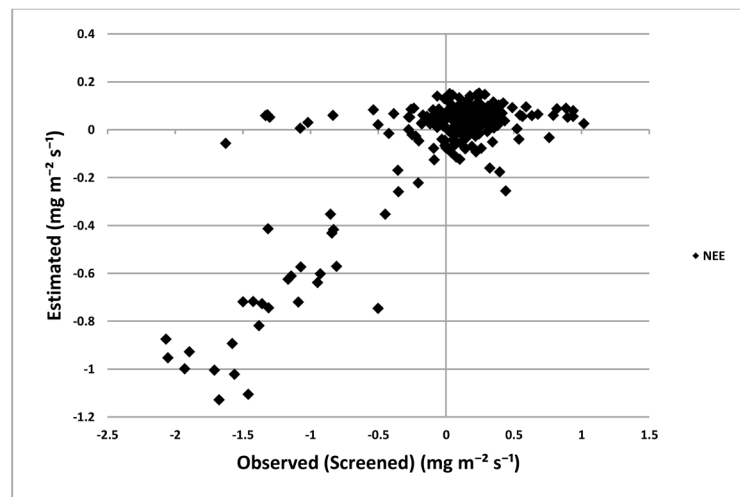
Table 5. Models evaluation.

Models	RMSE (mg·m ⁻² ·s ⁻¹)	MAE (mg·m ⁻² ·s ⁻¹)	e_{\max} (mg·m ⁻² ·s ⁻¹)
MLP (BP)	0.3881	0.2816	2.7724
RBF	0.3762	0.2635	2.5619
Papale	0.3285	0.2004	2.5301

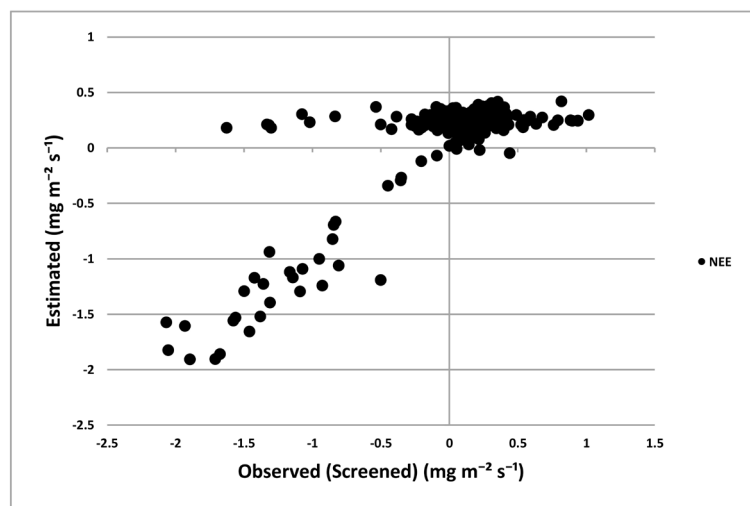
$$e_{\max} = |\text{Maximum Error Value} - \text{Minimum Error Value}|.$$



(a)

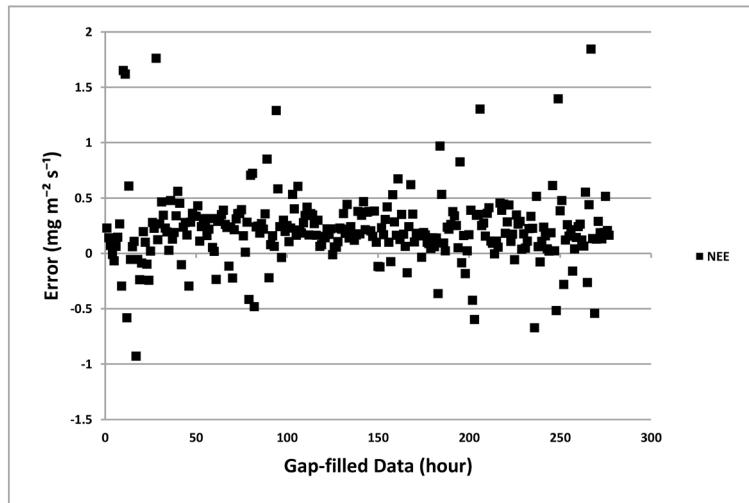


(b)

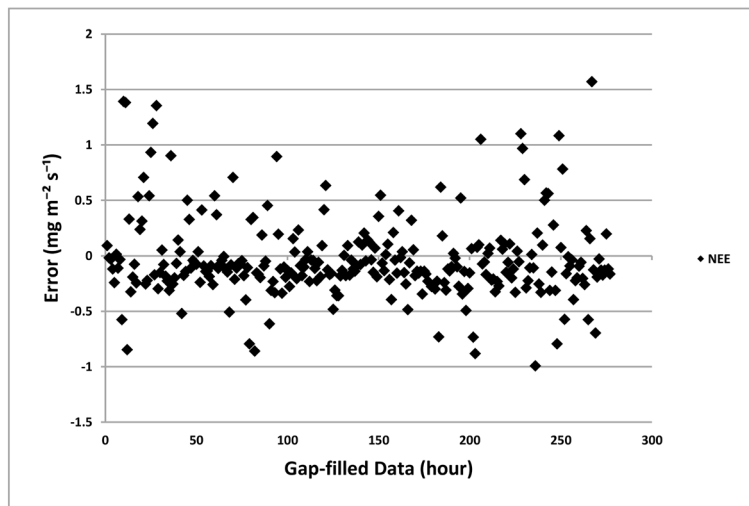


(c)

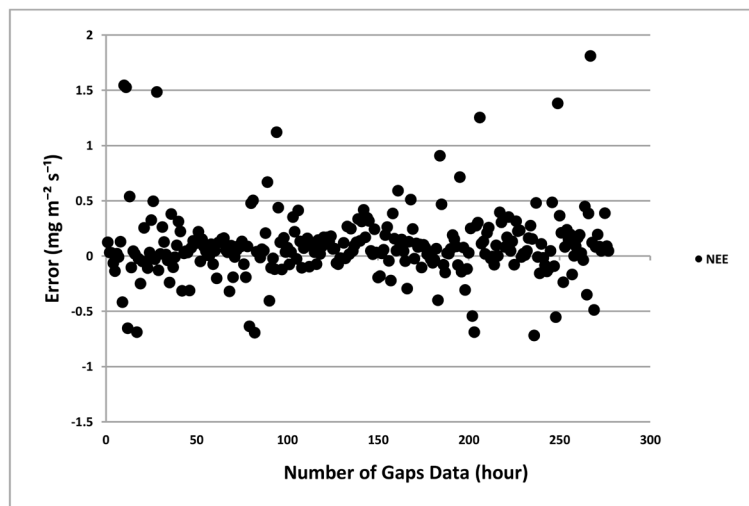
Figure 8. Estimation of NEE for observed (screened) values using (a) MLP (BP), (b) RBF and (c) Papale methods.



(a)

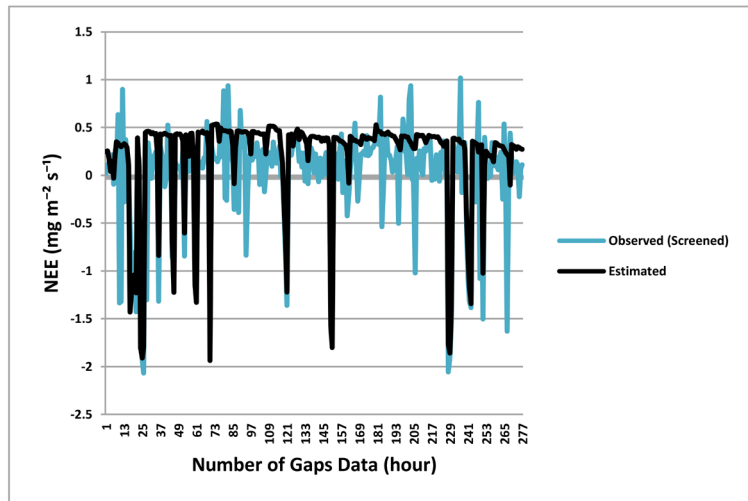


(b)

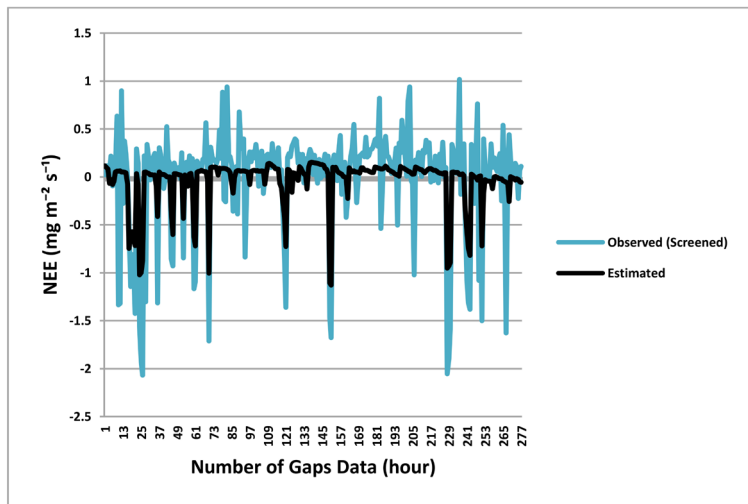


(c)

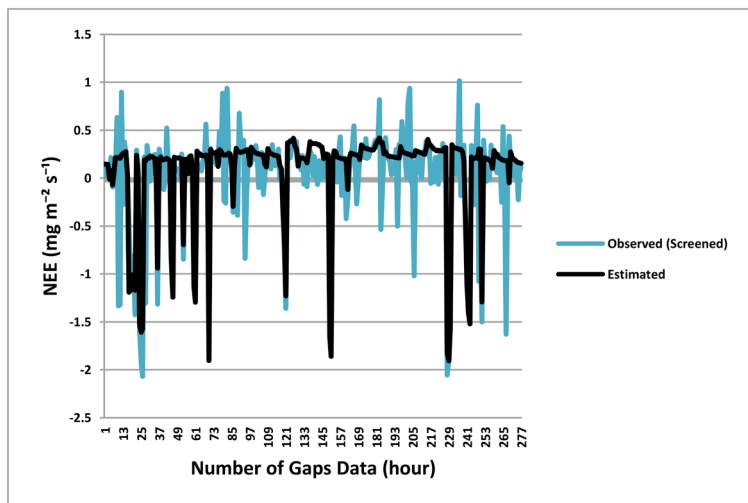
Figure 9. The difference (error) between estimated and observed (screened) values of NEE using (a) MLP (BP), (b) RBF and (c) Papale methods.



(a)



(b)

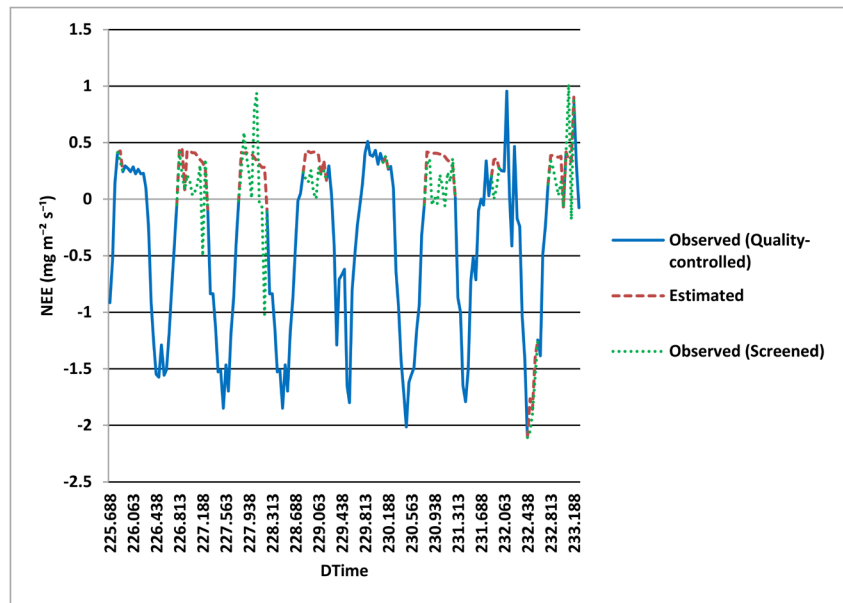


(c)

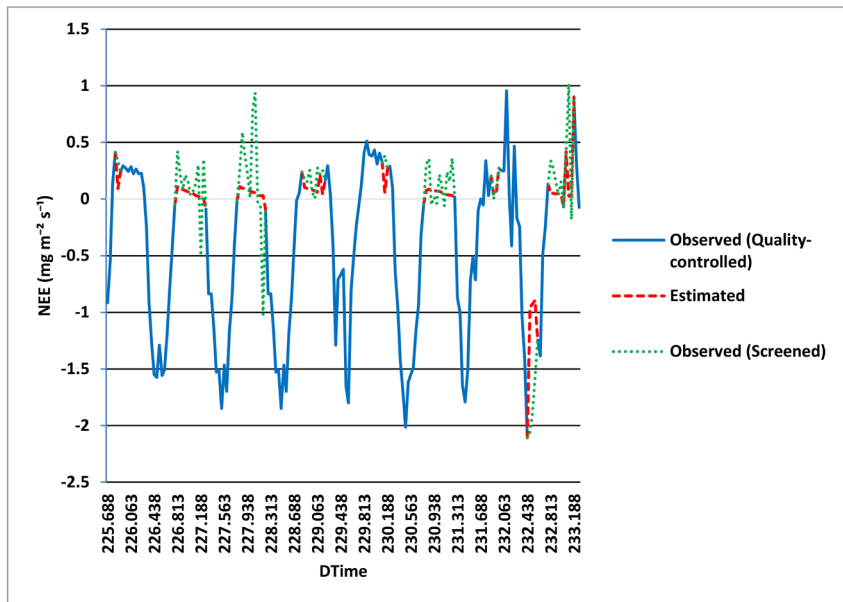
Figure 10. Comparison of estimated and observed (screened) values of NEE using (a) MLP (BP), (b) RBF and (c) Papale methods.

Figures 11(a)-(c) illustrate the observed (quality-controlled), estimated, and observed (screened) values for a short segment (5.5 days) of the NEE variation in 2005, using the applied methods. The representative time period is exactly the same as Figure 7. The remarkable difference between the Figure 11 and Figure 7 is due to the gap-filled data in daytime in Figure 11. It indicates that the applied techniques by Papale and Verma & Suyker for quality control of the data are dissimilar. This dissimilarity is the main reason that leads to the difference among the applied test and validated files by Papale and Verma & Suyker’s approach.

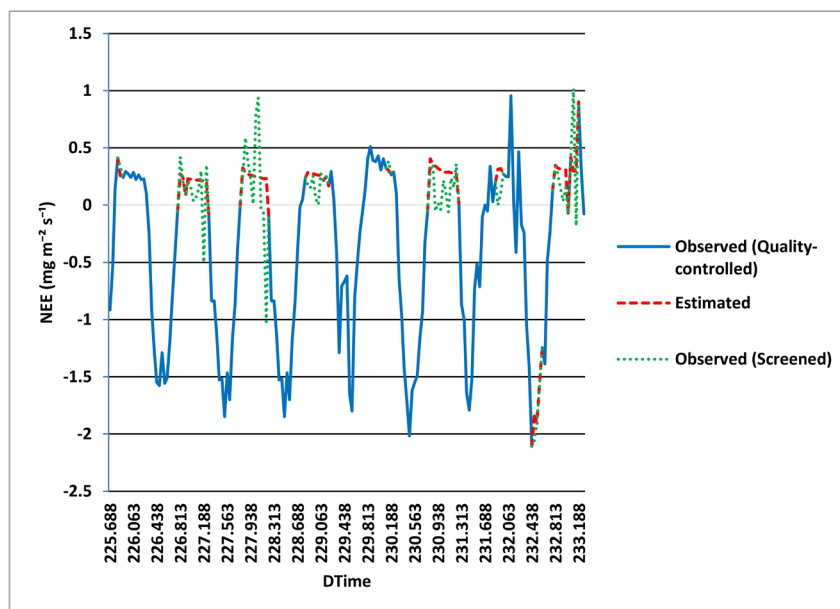
There may be several reasons that support Papale’s approach compared to our methods, such as input variables and network characteristics.



(a)



(b)



(c)

Figure 11. Comparison of the estimated and observed (quality-controlled and screened) values of NEE using (a) MLP (BP), (b) RBF and (c) Papale methods from local time of day 225.688 to 233.271.

Input variables: According to [8], air temperature, air relative humidity, photosynthetically active radiation (PAR), and two series of four fuzzy sets (transformation of season and time of day to numerical form). The CO₂ flux dataset used by Papale's approach contained 16 European sites (each site consisted of about 17,500 samples) within different climate zones and ecological parameters. Thus, using the larger data set (more samples) in order to train the network by Papale's approach promote the efficiency of his method compared to the other applied methods in this study.

Network characteristics: The dissimilarity in network architecture and parameters are influential factors on the model performance; though there is no information regarding the network architecture and parameters in the references.

4. Conclusions

Eddy covariance method is one of the best approaches to measure net ecosystem exchange flux above plant canopies. However, data collection using this method is prone to gaps. Today, several techniques are used to fill the missing data. In this study, the capability of the Multi-layer Perceptron (MLP) network trained by the Back-Propagation (BP) algorithm and the Radial Basis Function (RBF) network are compared with each other. Their results then are compared to Verma and Suyker's (V&S) method for the same time period.

The results confirmed the RBF network succeeded in the best fit for observed (screened) values based on statistical tests. Moreover, using a single method for gap-filling over a year was the advantage of the application of Artificial Neural

Networks (ANNs) compared to the V&S approach.

In the second part, the preference of RBF and MLP (BP) were compared to Papale's method, which fundamentally was also an ANN-based on MLP (BP). Results indicated that there was no striking difference among the three methods. Nevertheless, according to statistical indices, the Papale method was the best. Several reasons could be given for attaining the best estimation for NEE by Papale's method. One of them is the structure of data matrices, including both qualities and quantities. The network architecture and parameters are the other effective factors to this achievement.

Overall, the results show that ANNs, as a technique, is able to estimate the missing NEE data with good accuracy and efficiency.

Conflicts of Interest

The authors declare no conflicts of interest regarding the publication of this paper.

References

- [1] Verma, S.B., Dobermann, A., Cassman, K.G., Walters, D.T., Knops, J.M., Arkebauer, T.J., et al. (2005) Annual Carbon Dioxide Exchange in Irrigated and Rainfed Maize-Based Agroecosystems. *Agricultural and Forest Meteorology*, **131**, 77-96. <https://doi.org/10.1016/j.agrformet.2005.05.003>
- [2] Neal, A.L., Gupta, H.V., Kurc, S.A. and Brooks, P.D. (2011) Modeling Moisture Fluxes Using Artificial Neural Networks: Can Information Extraction Overcome Data Loss? *Hydrology and Earth System Sciences*, **15**, 359-368. <https://doi.org/10.5194/hess-15-359-2011>
- [3] Dragomir, C.M., Klaassen, W., Voiculescu, M., Georgescu, L.P. and van der Laan, S. (2012) Estimating Annual CO₂ Flux for Lutjewad Station Using Three Different Gap-Filling Techniques. *The Scientific World Journal*, **2012**, Article ID: 842893. <https://doi.org/10.1100/2012/842893>
- [4] Falge, E., Baldocchi, D.D., Olson, R., Anthoni, P., Aubinet, M., Bernhofer, C., et al. (2001) Gap Filling Strategies for Defensible Annual Sums of Net Ecosystem Exchange. *Agricultural and Forest Meteorology*, **107**, 43-69. [https://doi.org/10.1016/S0168-1923\(00\)00225-2](https://doi.org/10.1016/S0168-1923(00)00225-2)
- [5] Ruppert, J., Mauder, M., Thomas, C. and Lüers, J. (2006) Innovative Gap-Filling Strategy for Annual Sums of CO₂ Net Ecosystem Exchange. *Agricultural and Forest Meteorology*, **138**, 5-18. <https://doi.org/10.1016/j.agrformet.2006.03.003>
- [6] Moffat, A.M., Papale, D., Reichstein, M., Hollinger, D.Y., Richardson, A.D., Barr, A.G., et al. (2007) Comprehensive Comparison of Gap-Filling Techniques for Eddy Covariance Net Carbon Fluxes. *Agricultural and Forest Meteorology*, **147**, 209-232. <https://doi.org/10.1016/j.agrformet.2007.08.011>
- [7] Suyker, A.E., Verma, S.B. and Burba, G.G. (2003) Interannual Variability in Net CO₂ Exchange of a Native Tallgrass Prairie. *Global Change Biology*, **9**, 255-265. <https://doi.org/10.1046/j.1365-2486.2003.00567.x>
- [8] Papale, D. and Valentini, R. (2003) A New Assessment of European Forests Carbon Exchanges by Eddy Fluxes and Artificial Neural Network Spatialization. *Global Change Biology*, **9**, 525-535. <https://doi.org/10.1046/j.1365-2486.2003.00609.x>

- [9] Safa, B., Khalili, A., Teshnehlab, M. and Liaghat, A. (2011) Artificial Neural Networks Application to Predict Wheat Yield Using Climatic Data. *Journal of Agricultural Science and Technology B*, **1**, 76-88.
- [10] Schmidt, A., Wrzesinsky, T. and Klemm, O. (2008) Gap Filling and Quality Assessment of CO₂ and Water Vapor Fluxes above an Urban Area with Radial Basis Function Neural Networks. *Boundary-Layer Meteorology*, **126**, 389-413. <https://doi.org/10.1007/s10546-007-9249-7>
- [11] Salehi, F., Lacroix, R. and Wade, K.M. (1998) Effects of Learning Parameters and Data Presentation on the Performance of Back-Propagation Networks for Milk Yield Prediction. *Trans. ASAE*, **41**, 253-259. <https://doi.org/10.13031/2013.17144>
- [12] Kumar, M., Raghuvanshi, N.S., Singh, R., Wallender, W.W. and Pruitt, W.O. (2002) Estimating Evapotranspiration Using Artificial Neural Network. *Journal of Irrigation and Drainage Engineering*, **128**, 224-233. [https://doi.org/10.1061/\(ASCE\)0733-9437\(2002\)128:4\(224\)](https://doi.org/10.1061/(ASCE)0733-9437(2002)128:4(224))
- [13] Bors, A. (2001) Introduction of the Radial Basis Function (RBF) Networks. *Online Symp. Electron. Eng*, **1**, 1-7.
- [14] Fidêncio, P.H., Poppi, R.J. and de Andrade, J.C. (2002) Determination of Organic Matter in Soils Using Radial Basis Function Networks and Near Infrared Spectroscopy. *Analytica Chimica Acta*, **453**, 125-134. [https://doi.org/10.1016/S0003-2670\(01\)01506-9](https://doi.org/10.1016/S0003-2670(01)01506-9)
- [15] Hajjiha, A., Branch, N.T. and Branch, K. (2006) Improving Behavioral Based Job Assignment by Using Radial Basis Function Network. *Proceedings of the 6th WSEAS International Conference on Systems Theory & Scientific Computation*, Elounda, 21-23 August 2006, 64-69.
- [16] Karimi, B., Menhaj, M.B. and Saboori, I. (2006) Robust Adaptive Control of Nonaffine Nonlinear Systems Using Radial Basis Function Neural Networks. *IECON 2006 32nd Annual Conference on IEEE Industrial Electronics*, Paris, 6-10 November 2006, 495-500. <https://doi.org/10.1109/IECON.2006.347327>
- [17] Aslani, G., Momeni-Masuleh, S.H., Malek, A. and Ghorbani, F. (2009) Bank Efficiency Evaluation Using a Neural Network-DEA Method. *Iranian Journal of Mathematical Sciences and Informatics*, **4**, 33-48.
- [18] Halici, U. (1994) Hints from Life to Artificial Intelligence. Middle East Technical University, Ankara, 139-147.
- [19] Kisi, Ö. (2009) Daily Pan Evaporation Modelling Using Multi-Layer Perceptrons and Radial Basis Neural Networks. *Hydrological Processes*, **23**, 213-223. <https://doi.org/10.1002/hyp.7126>
- [20] Foken, T. and Wichura, B. (1996) Tools for Quality Assessment of Surface-Based Flux Measurements. *Agricultural and Forest Meteorology*, **78**, 83-105. [https://doi.org/10.1016/0168-1923\(95\)02248-1](https://doi.org/10.1016/0168-1923(95)02248-1)
- [21] Moody, J. and Darken, C. (1989) Fast Learning in Networks of Locally-Tuned Processing Units. *Neural Computation*, **1**, 281-294. <https://doi.org/10.1162/neco.1989.1.2.281>
- [22] Braswell, B.H., Sacks, W.J., Linder, E. and Schimel, D.S. (2005) Estimating Diurnal to Annual Ecosystem Parameters by Synthesis of a Carbon Flux Model with Eddy Covariance Net Ecosystem Exchange Observations. *Global Change Biology*, **11**, 335-355. <https://doi.org/10.1111/j.1365-2486.2005.00897.x>